Algorithmic design and implementation considerations of deep MPC

Prabhat K. Mishra, Mateus V. Gasparino, and Girish Chowdhary

Abstract—Deep Model Predictive Control (Deep MPC) is an evolving field that integrates model predictive control and deep learning. This manuscript is focused on a particular approach, which employs deep neural network in the loop with MPC. This class of approaches distributes control authority between a neural network and an MPC controller, in such a way that the neural network learns the model uncertainties while the MPC handles constraints. The approach is appealing because training data collected while the system is in operation can be used to fine-tune the neural network, and MPC prevents unsafe behavior during those learning transients. This manuscript explains implementation challenges of Deep MPC, algorithmic way to distribute control authority and argues that a poor choice in distributing control authority may lead to poor performance. A reason of poor performance is explained through a numerical experiment on a four-wheeled skid-steer dynamics.

I. INTRODUCTION

Deep learning-based MPC utilizes the constraint satisfaction capability of MPC and the function approximation capability of *Deep Neural Network* (DNN). It is evident that machine learning and deep learning techniques can enhance the performance of MPC. However, there is still a lack of successful results demonstrating the use of deep learning to augment MPC policies in uncertain environments, employing deep neural networks (DNNs) to learn uncertainties online [1]. One of the results to address such problem was reported in [2].

Deep MPC [2] is based on Tube-MPC [3] and inherits mathematical analysis from tube-MPC itself, which guarantees input-to-state stability of the controlled system. In addition, the idea of [2] is based on collecting the training data for DNN online while the system is in operation and the training data is collected from a DNN itself, similar to [4]. This mechanism is summarized in Fig. 1 and will be discussed in more detail later.

To integrate a DNN within the tube-MPC framework, it is essential that the DNN produces bounded outputs. This allows MPC to treat the DNN output as an additional bounded disturbance [5]. This requirement can be addressed by using bounded activation functions in the output layer and constraining the weights (trainable parameters of the outermost layer) through projection onto a bounded set. While it may seem that bounding the weights of the output layer is necessary solely because tube-MPC is designed to

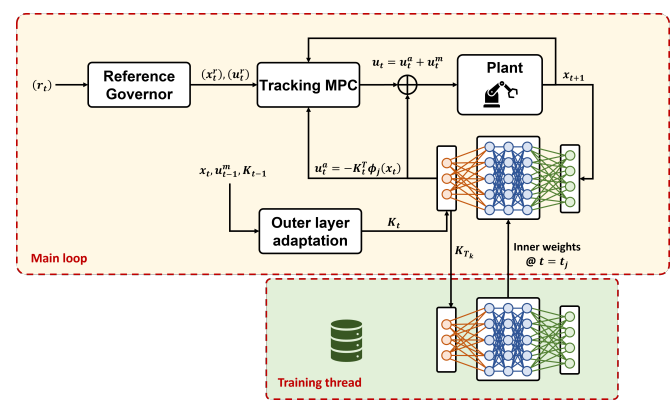


Fig. 1: Deep MPC has a neural network in the loop with MPC in which the outermost layer is adapted at each time instant and its output is stored in a replay buffer to create training dataset to train its inner layers intermittently in a remote training thread.

handle only bounded disturbances (i.e., the DNN outputs), this constraint is also crucial for mitigating the parameter drift phenomenon commonly encountered in adaptive control

Parameter drift phenomenon also reminds the crash of X-15 in October 1967 in which the pilot Michael Adams died and due to the incident flight testing of adaptive control stopped for around the next thirty years [6]. However, several new methods of robust adaptive control have also been developed later. One of the approaches to avoid the parameter drift phenomenon is based on projecting the learned weights on a bounded set.

In the context of Deep MPC [2], the output of a DNN itself is used to train another DNN. Therefore, the output dataset of a DNN with projected weights and bounded activation function results in vanishing gradient phenomenon during the training. As a result, in many cases performance of tube-MPC and deep MPC either remains the same or in some cases the underlying optimization problem of deep MPC becomes infeasible. In particular, let $u_t := u_t^a + u_t^m$ be the control applied at time t, where u_t^a is the learning component and u_t^m is the MPC component. Since u_t should be bounded for all t, a careful distribution of control authority between u_t^a and u_t^m is required. When u_t^a does not get enough control authority, learning may not happen and therefore, their performance may be the same. When u_t^m does not get enough control authority, the underlying optimization problem can become infeasible. This manuscript provides a tutorial introduction to Deep MPC, its algorithmic details and provides numerical justification about distributing the control authority between u_t^a and u_t^m .

P. K. Mishra is with the Department of Artificial Intelligence at Indian Institute of Technology, Kharagpur, India. (pkmishra@ai.iitkgp.ac.in).

M. V. Gasparino is with the University of Illinois at Urbana Champaign (UIUC), IL, USA. The publication was written prior to M. V. Gasparino joining Amazon.

G. Chowdhary is with the University of Illinois at Urbana Champaign (UIUC), IL, USA (girishc@illinois.edu).

Our notations are standard and mostly defined before their first use. We describe the problem setup in §II and provide the overall architecture of deep MPC in §III. The implementation details, algorithms and explanations are provided in §IV. The reason of poor learning in deep MPC is explained through a numerical experiment in §V and finally we conclude in §VI.

II. PROBLEM SETUP

We are interested in a dynamics, which has the form

$$x_{t+1} = f(x_t) + g(x_t) (u_t + h(x_t)), \tag{1}$$

where

- (1-a) $x_t \in \mathcal{X} \subset \mathbb{R}^d$, $u_t \in \mathcal{U} \subset \mathbb{R}^m$ are state and action, respectively, at time t.
- (1-b) The term $g(x_t)h(x_t)$ represents state-dependent disturbance and there exists $w_{\max} > 0$ such that $\|g(x)h(x)\| \le w_{\max}$ for all $x \in \mathcal{X}$.
- (1-c) The functions f and g are known and Lipschitz continuous.
- (1-d) The function h is unknown but continuous 1,
- (1-e) X and U are compact sets.
- (1-f) The matrix g(x) is left invertible for each $x \in X$.

There are many practical applications where an uncertain system follows the recursion (1). In a practical continuous-time system such as mobile robots, digital controllers can be implemented by either discretizing the dynamics before computing the control or discretizing the controller before implementing it. Optimal control formulations such as reinforcement learning and MPC are generally based on discretized dynamics while adaptive control implementations are generally based on discretized controller.

In some cases we may be interested in a control constraint of the form $|u_t^i| \le u_{\max}^i$ for $i = 1, \dots, m$. These constraints can be written in the form $||u_t||_{\infty} \le u_{\max}$ by scaling $g(x_t)$ [8, Remark 1]. Therefore, for simplicity, we define $\mathcal{U} := \{u \in \mathbb{R}^m \mid ||u||_{\infty} \le u_{\max}\}$.

The deep MPC [2] control u_t has two components namely a learning component u_t^a and a MPC component u_t^m . The composite control $u_t = u_t^a + u_t^m$ is applied to the system. In the problem setup, we have assumed $h: X \to \mathbb{R}^d$ is continuous and X is compact. Therefore, h(x) will be bounded for all $x \in X$. Since $h(x_t)$ is additive to u_t , we can think about designing $u_t^a = -h(x_t)$, if possible. Since h is unknown, we are interested in learning u_t^a . The term u_t^m should be used to fulfil other control objectives such as regulating states from a given state to a desired state. Since the control authority is limited by the constraint $||u_t||_{\infty} \leq u_{\max}$, we need to redistribute the control authority u_{\max} between u_t^a and u_t^m .

In the next section, we will describe the overall deep MPC architecture, then focus on the implementation details, specially how the control authority can be distributed between u_t^a and u_t^m algorithmically.

III. DEEP MPC

The overall deep MPC architecture consists of a reference governor, tracking MPC, adaptation mechanism and two neural networks as shown in Fig. 1. Both neural networks have the same architecture with one linear output layer followed by a layer with bounded activation functions such as Tanh, sigmoidal, etc. The remaining architecture of the neural networks is flexible and the choice depends on the type of problems. For simplicity, we can consider fully connected layers too.

Reference governor and tracking MPC modules are same as tube MPC [3] with modifications required to adjust the adaptation mechanism. In other words, to steer a dynamical system (1) from the initial state x_0 to the target state x^s while satisfying the state and action constraints described with (1), we are interested in designing the control $u_t = u_t^a + u_t^m$ at time t, where u_t^a is the output of the neural network in the main loop; please see Fig. 1. Reference governor takes slowly varying reference r_t as input and suggests a trajectory from x_0 to r_t . For simplicity, we consider $r_t = x^s = 0$, which means the reference governor is designed offline for a regulation problem. For a tracking problem, reference governor is invoked whenever r_t changes [3], [9]. The trajectory generated by reference governor need to have sufficient margin from the boundaries of X so that the states of the uncertain system (1) controlled by the tracking MPC stay in X. Therefore, tightening of constraints before designing the reference governor is required, which will be discussed in the next section.

The adaptation mechanism as shown in Fig. 1 updates the parameters of the output layer (wights and biases) by assuming the hidden layers as a fixed feature basis function. Since the ideal feature basis function is not known in case of unstructured uncertainties, we utilize the second neural network. To train this second neural network, we use the data available in the replay buffer. To create the replay buffer data, we use output of neural network (main loop) as label and corresponding state as input with some experience selection criterion [10]. We can intermittently (at time instants $(t_j)_{j \in \mathbb{N}}$) replace the parameters of the hidden layers of neural network (main loop) by the parameters of the hidden layers of the second neural network.

IV. IMPLEMENTATION DETAILS OF DEEP MPC

We have assumed that the state-dependent additive disturbance $||g(x)h(x)|| \le w_{\max}$ for all $x \in \mathcal{X}$. We can consider the set \mathcal{X} as our intended region of operation. Once we have a discrete dynamics (1), the next step to implement deep MPC is the computation of some acceptable value of w_{\max} .

Most of the commercial devices come with their ratings. Therefore an acceptable value of $w_{\rm max}$ can be safely prescribed. For example, the maximum crosswind speed for an air-plane is prescribed in its flying handbook [11, Chapter 9]. Related discussion about the Boeing aircraft is provided in the report [12]. When such bounds are not provided by the manufacturer, specially when the device is assembled in the laboratory, experiments can be performed to compute bounds similar to the approach available in [13, Fig. 6]. As an example consider that 36 kts is provided as the maximum crosswind

¹The term h(x) is considered state-dependent matched uncertainty at the state x. Refer to [7] for the definitions of matched and unmatched uncertainties.

speed as company policy for landing but it can also vary according to the runway conditions. Consider a case as another example where a drone is tasked with delivering packages in an urban environment. Suppose initial experiments reveal that the position estimation error varies between 1 and 5 meters due to GPS signal interference in different urban settings. After consulting with domain experts, if the control engineer finds that the signal can be further degraded by certain environmental features like tall buildings or dense foliage, etc., they can prescribe a larger error bound (say 6 meters) and design the controller accordingly. For more algorithmic clarity and generalization of the approach, we can use data generation methods as discussed in [14, Chapter 2]. Suppose we have M trajectories containing (x_t, u_t) pairs and T_i denotes the length of i^{th} trajectory. We can follow the Algorithm 1 to compute w_{max} and u_{max}^a , where the variable u_{max}^a will be discussed in the context of learning in more detail and for our own understanding, we can call it a learning authority, i. e. $||u_t^a||_{\infty} \le u_{\max}^a$ for all t.

Algorithm 1 Computation of bounds $w_{\text{max}}, u_{\text{max}}^a$

```
1: Input: (x_j, u_j)_{j=0}^{T_i} for i = 1, ..., M, f, g

2: Output: w_{\text{max}}, u_{\text{max}}^a

3: w_{\text{max}}, u_{\text{max}}^a \leftarrow 0

4: for i \leftarrow 1 to M do

5: for j \leftarrow 0 to T_i - 1 do

6: w \leftarrow x_{j+1} - f(x_j) - g(x_j)u_j

7: w^a \leftarrow g(x_j)^{\dagger}w

8: w_{\text{max}} \leftarrow \max\{w_{\text{max}}, w\}

9: u_{\text{max}}^a \leftarrow \max\{u_{\text{max}}^a, w^a\}

10: return w_{\text{max}}, u_{\text{max}}^a
```

Now we need to design a reference governor. Reference governor provides a trackable reference trajectory, which can be tracked by the nominal dynamics. To clear the nomenclature, we can call (1) our uncertain dynamics because it has an unknown term $h(x_t)$. The nominal dynamics is given by $x_{t+1} = f(x_t) + g(x_t)u_t^m =: \bar{f}(x_t, u_t^m)$. We can also use other names for the nominal dynamics such as simulator dynamics or the dynamics of the digital twin. In a regulation problem, if our set-point is (x^s, u^s) such that $x^s = f(x^s) + g(x^s)u^s$ and the starting point x_0 is given, our control objective is to reach the set-point without violating the state and action constraints while minimizing some cost. We emphasize the definition of set-points for beginners because in most of the cases $u^s = 0$ may not serve the purpose. For example, in order to maintain the temperature of a room at certain level x^s , a certain amount of heating u^s is required. Role of reference governor is to suggest a trajectory from x_0 to x_s such that we can find $u_t \in \mathcal{U}$, which can maintain the states of the uncertain system (1) in the operational region X. Since the reference governor works on the nominal dynamics, we tighten the sets X and \mathcal{U} . This approach is called constraint tightening and is an active area of research in MPC [15]-[18]. For linear dynamical systems, the tightened constraint set X_r can be obtained by various types of robust positively invariant (RPI) sets by using different

methods such as subtracting the evolution of the disturbance set from the set \mathcal{X} . These methods provide analytic expression of the tightened sets but they involve polytopic set computations and are therefore, computationally expensive. In practical implementations generally some approximation of RPI set or tightened set is used. For non-linear dynamical systems, constraint tightening is more difficult not only computationally but also analytically.

As discussed in [3, §7], constraints of the system (1) are satisfied by the tightening the constraints of the nominal dynamics \bar{f} used in the design of the reference governor and then forcing the states and control of the online MPC in a tube. The online MPC has constraints only on control, so the satisfaction of state constraints solely depend on the constraint tightening. Theoretical results guarantee that the states of the controlled system lie in a tube defined by level sets, which is defined in terms of the value function of the online MPC [2, Proposition 1].

Constraint tightening plays a very important role in tube-based MPC formulation and the intuition is that when the nominal dynamics satisfy the tightened constraints, the uncertain dynamics will satisfy the constraints given in (1). Since deep MPC has to distribute control authority between MPC component and learning component, we define $\bar{\mathcal{U}} := \{u \in \mathbb{R}^m \mid \|u\|_{\infty} \leq u_{\max} - u_{\max}^a\}$ and compute the tightened control set $\mathcal{U}_r \subset \bar{\mathcal{U}}$ according to [3, §7].

Once we have tightened sets $X_r \subset X$ and $\mathcal{U}_r \subset \bar{\mathcal{U}}$, we can solve a finite horizon problem by using the nominal dynamics $\bar{f}(x_t, u_t^m) = f(x_t) + g(x_t)u_t^m$ as follows:

$$\min_{\substack{(u_i^r)_{i=0}^{N-1}\\ i=0}} \sum_{i=0}^{N-1} \|x_i^r\|_Q^2 + \|u_i^r\|_R^2$$
s. t.
$$x_0^r = x_0, x_N^r = \mathbf{0}, \\
x_{i+1}^r = \bar{f}(x_i^r, u_i^r) \in \mathcal{X}_r \subset \mathcal{X}, \\
x_i^r \in \mathcal{U}_r \subset \bar{\mathcal{U}}; i = 0, \dots, N-1,$$
(2)

to generate a reference trajectory $(x_t^r, u_t^r)_{t=0}^N$, where N is the optimization horizon. The design of reference governor is popular for designing hierarchical MPC to satisfy constraints [19]. We can use CasADi [20] to design a reference governor by using the algorithm 2.

Algorithm 2 Reference governor

```
1: Input: N, Q, R, x_0, x^s, u^s, X_r, \mathcal{U}_r, \bar{f}

2: Output: (x_t^r, u_t^r)_{t=0}^N

3: x_0 = x_0 - x^s

4: Solve (2)

5: x_t^r \leftarrow x_t^r + x^s, u_t^r \leftarrow u_t^r + u^s

6: return (x_t^r, u_t^r)_{t=0}^N
```

The MPC component u_t^m in Deep MPC is aware of the learning component u_t^a , therefore we need to design u_t^a before u_t^m . As depicted in Fig. 1 that the outermost layer of the neural network is updated at each time instant by keeping the inner layers fixed. The deep MPC approach allows the training of inner layers intermittently. Let k^{th} training of inner layers starts

at the time instant T_k and j^{th} training finishes before the time instant t_j . We initialize K_0 such that $\left\|K_0^{(i)}\right\| \le \bar{W}_i; i = 1, ..., m$. For a given learning rate $0 < \theta < 1$ and for $t \in \{t_j + 1, ..., t_{j+1}\}$, we employ the following weight update law:

$$\bar{K}_t = K_{t-1} + \frac{\theta}{\left\|\phi_j(x_{t-1})\right\|^2} \phi_j(x_{t-1}) \left(g(x_{t-1})^{\dagger} (x_t - \bar{f}(x_{t-1}, u_{t-1}^m))\right)^{\top}, \text{ The overall deep MPC algorithm is given in Algorithm 4.}$$

where $g(x_{t-1})^{\dagger} = (g(x_{t-1})^{\top} g(x_{t-1}))^{-1} g(x_{t-1})^{\top}$ represents the pseudo-inverse of the left invertible matrix $q(x_{t-1})$. The above weight update law has been derived in [21] for structured uncertainties and has been used in [22] along with MPC. Notice that the first element in $\phi_i(\cdot)$ is one. Therefore, $\|\phi_i(x)\|^2 \ge 1$ for all $x \in \mathbb{R}^d$ and $j \in \mathbb{N}_0$, which avoids any possibility of division by zero. We employ the discrete projection method to ensure boundedness of $K_t^{(i)}$ for i = 1, ..., m, as follows:

$$K_{t}^{(i)} = \operatorname{Proj} \bar{K}_{t}^{(i)} = \begin{cases} \bar{K}_{t}^{(i)} & \text{if } \left\| \bar{K}_{t}^{(i)} \right\| \leq \bar{W}_{i} \\ \frac{\bar{W}_{i}}{\left\| \bar{K}_{t}^{(i)} \right\|} \bar{K}_{t}^{(i)} & \text{otherwise.} \end{cases}$$
(4)

Algorithm 3 Transfer learning in the neural network for $t \in$ $[t_j, t_{j+1}[$

```
1: Input: x_t, x_{t-1}, u_{t-1}^m, \bar{f}, \phi_j, \bar{W}_i for i = 1, ..., m
2: Output: K_t \triangleright Weights of the output layer
```

3: update (3)

4: projection (4)

5: return K_t

The Algorithm 3 provides K_t for $t \in \{t_i + 1, ..., t_{j+1}\}$ and is used to generate the learning component $u_t^a = -K_t^{\mathsf{T}} \phi_i(x_t)$ for $t \in \{t_j, \dots, t_{j+1} - 1\}$. The pair (x_t, u_t^a) are stored in a replay buffer for the supervised fine tuning of the neural network on the basis of some experience selection criterion [10], [23]. The Algorithm 3 has also been used in [24].

Once all these modules are ready, we can create the main module of deep MPC. In order to design the online reference tracking MPC, we first choose symmetric positive definite matrices $Q, R \succ \mathbf{0}$, which can be different from those chosen for the reference governor. Let $c_s(x_{t+i|t}, u_{t+i|t}) :=$ $\|x_{t+i|t} - x_{t+i}^r\|_Q^2 + \|u_{t+i|t} - u_{t+i}^r\|_R^2$ be the cost per stage at time t+i predicted at time t and let $c_f(x) := x^\top Q_f x$ be the terminal cost with $Q_f > 0$.

Let us define

$$V_m(x_{t|t}, (u_{t+i|t})_{i=0}^{N-1}) \coloneqq c_f(x_{t+N|t}) + \sum_{i=0}^{N-1} c_s(x_{t+i|t}, u_{t+i|t}).$$
(5)

The online reference tracking MPC minimizes (5) at each time instant t under the following constraints:

$$x_{t|t} = x_t \tag{6}$$

$$u_{t|t} + u_t^a \in \mathcal{U} \tag{7}$$

$$x_{t+i+1|t} = f(x_{t+i|t}) + g(x_{t+i|t})u_{t+i|t}$$
 for $i = 0, \dots, N-1$ (8)

$$u_{t+i|t} \in \bar{\mathcal{U}} \text{ for } i = 1, \cdots, N-1.$$
 (9)

Notice that the constraint (7) is different from the constraints present in tube-MPC formulation [3]. We define the underlying optimal control problem

$$V_m(x_t) := \min_{(u_{t+i|t})_{i=0}^{N-1}} \left\{ (5) \mid (6), (7), (8), (9) \right\}. \tag{10}$$

```
Algorithm 4 Deep MPC
```

```
1: Input: X, \mathcal{U}, x^s, u^s, \{t_i\}, \{T_k\}, replay buffer
 2: Output: u<sub>t</sub>
 3: Compute w_{\text{max}}, u_{\text{max}}^a by Algorithm 1
 4: Constraint tightening according to [3, §7]
 5: Generate the reference trajectory (x_t^r, u_t^r) by Algorithm 2
 6: for each t do
7:
         measure state x_t
         if t = T_k then
 8:
9:
              activate the training thread
10:
              take random samples from the replay buffer
              freeze output layer weights to be K_{T_k}
11:
              train the network
12:
              k \leftarrow k + 1
13:
         Compute K_t by Algorithm 3
14:
         if t = t_i then
15:
16:
              update \phi_i in the main loop
              j \leftarrow j + 1
17:
         u_t^a = -K_t^{\top} \phi_i(x_t)
18:
         if (x_t, u_t^a) satisfies the experience selection criterion
19:
    then
              Store (x_t, u_t^a) in the replay buffer
20:
         Solve (10) to get u_t^m
21:
         return u_t = u_t^a + u_t^m
22:
         t \leftarrow t + 1
23:
```

V. Numerical experiment

We consider a continuous time simplified non-slip fourwheeled skid-steer dynamics of the robot, which is used in [2], [25], [26] for robot navigation in an agricultural crop field. The states of the robots are represented by $s := \begin{bmatrix} x & y & \theta & v & \omega \end{bmatrix}$, where $x \in [-2, 1]$ is the robot's longitudinal position across the lane, $y \in [-0.5, 0.5]$ is the lateral position (cross-track error), $\theta \in [-\pi/2, \pi/2]$ is the heading angle with respect to the lane, $v \in [-1.5, 1.5]$ is the difference between the speed of the robot and the reference speed $v_r = 0.8$, and $\omega \in [-3,3]$ is the robot's angular rate. The control $u := [F_L \quad F_R]^{\top}$, where $F_L, F_R \in [-10, 10]$ are the left and right exerted forces used to move the robot's wheels. The continuous time dynamics is given by

$$\begin{bmatrix} \dot{x} \\ \dot{y} \\ \dot{\theta} \\ \dot{v} \\ \dot{\omega} \end{bmatrix} = \begin{bmatrix} (v+v_r)\cos\theta \\ (v+v_r)\sin\theta \\ \omega \\ 0 \\ 0 \end{bmatrix} + \begin{bmatrix} 0 & 0 \\ 0 & 0 \\ 0 & 0 \\ \frac{1}{M} & \frac{1}{M} \\ -\frac{b}{2} & \frac{b}{2} \end{bmatrix} \left(\begin{bmatrix} F_L \\ F_R \end{bmatrix} - R \right), \quad (11)$$

where the constants M = 15, I = 0.1, and b = 0.1 are the robot's physical properties that correspond to the mass, moment of

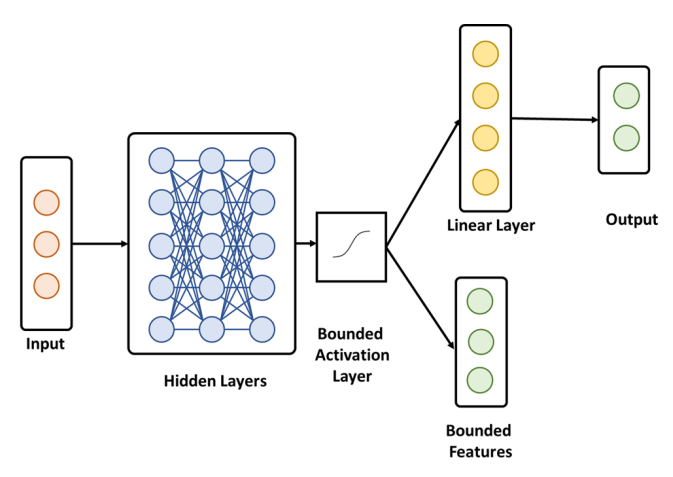


Fig. 2: The neural network architecture used in Deep MPC.

inertia, and distance between wheels. The continuous time dynamics is discretized by using the sampling time $T_s = 0.05$ seconds to get the dynamics of the form (1).

The matched uncertainty h(s) := -R represents unknown rolling resistance forces. For the purpose of simulation, we have generated R by using the expression $R^{(1)} = -2\cos\theta + \omega y - v\theta + \omega$ and $R^{(2)} = 2(1-\sin\theta) + xv - y - 0.5y^2$ as in [2]. The control objective is to steer the states of robot s_t from $s_0 = \begin{bmatrix} -1 & -0.25 & \pi/4 & 0 & -\pi/8 \end{bmatrix}^{\mathsf{T}}$ to the equilibrium $s_e = \begin{bmatrix} 0 & 0 & 0 & -v_r & 0 \end{bmatrix}$.

To design the deep MPC, we used a neural network with three hidden layers of sizes $\{8, 12, n_2\}$, where $n_2 = 4$ represents the outermost layer. We used tanh as a bounded activation function in the last hidden layer and Rectified Linear Unit (ReLU) in the remaining hidden layers; see Fig. 2. The weights of the linear output layer are updated by using (3) and (4) with learning rate $\theta = 0.5$ and bounds \bar{W}_i in (4) is obtained by

$$\bar{W}_i = \frac{u_{\text{max}}^a}{\sqrt{n_u(1 + 0.25n_2)}} \text{ for } i = 1, \dots, n_u + 1.$$
 (12)

The hidden layers of Deep MPC are trained at each 20 time steps using SGD with learning rate 0.01. We choose the optimization horizon N=10, the state penalty matrix Q as a diagonal matrix with entries $\{0.5,2,1,0.5,5\}$, the control penalty matrix R=I and the terminal cost matrix $Q_f=10^5I$. We have implemented the reference governor (2) by using the same parameters Q,R as the online MPC, N=100 and heuristically tightened the constraints by multiplying them with a factor of 0.9. We follow the approach of [23] for the inclusion and removal of data pairs based on the singular value maximization criterion. We carried out simulations by using a MATLAB-based software package MPCTools [27].

In this section, we have chosen $u_{\text{max}}^a = 0.6$ and experimental results are demonstrated in Fig. 3 and Fig. 4 for 100 time steps. Fig. 3 demonstrates that the trajectory of tube-MPC and deep MPC are very close to each other due to the absence of enough learning authority. The term $\tilde{u}_t = u_t^a + h(s_t)$ in Fig. 4 does not converge to some neighbourhood of origin instead it follows the trajectory of h(s) with some offset. This phenomenon is due to the saturation of the learning control u_t^a as shown in Fig.

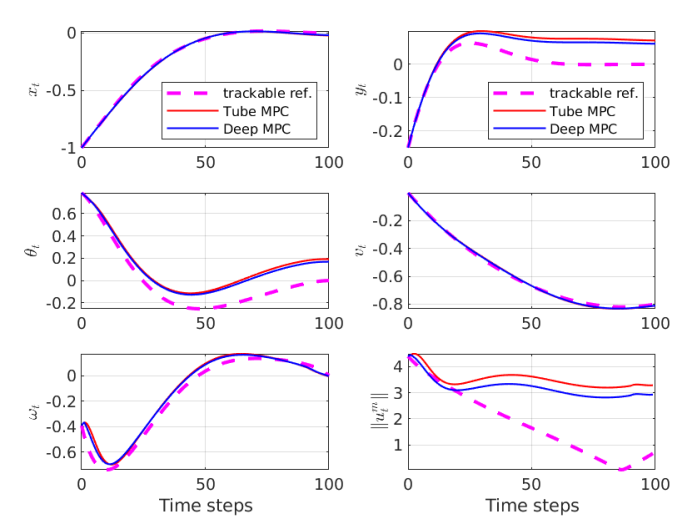


Fig. 3: In the absence of enough learning authority, performance of Deep MPC is close to that of tube MPC.

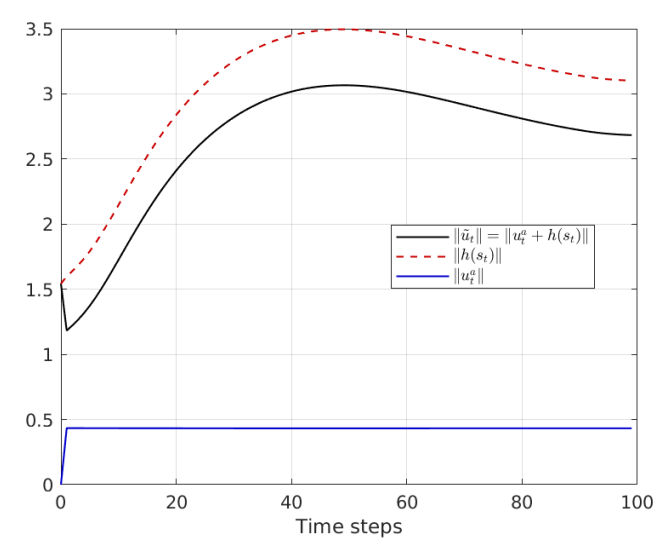


Fig. 4: In the absence of enough learning authority, u^a become saturated and therefore, $\tilde{u} = h + u^a$ changes according to h.

4. This experiment concludes that learning is not happening due to the absence of enough learning authority and saturation of the training data u_t^a resulting in the lack of relationship between x_t and u_t^a . For practical purposes, we can use u_{max}^a little larger or equal to the value obtained by using Algorithm 1, similar to the numerical experiment in [2].

We considered the same numerical experiment as in [2] but we chose smaller u_{max}^a and demonstrated that deep MPC performs as tube-MPC (Fig. 3). We explained the reason of not getting advantage over tube-MPC in Fig. 4. The simulation result reveals that smaller u_{max}^a leads to saturation of u_t^a and therefore learning does not happen.

VI. CONCLUSIONS

We have discussed about algorithmic implementation details of deep MPC. We have demonstrated through a numerical experiment that the poor choice of learning authority leads to poor performance. Future work may involve further simplification of constraint tightening or different approaches to satisfy state constraints. Evaluation of deep MPC for more challenging problems with different neural network architectures and experience selection criterion can be an interesting direction. The deep MPC algorithm is not suitable for random uncertainties but its integration with stochastic MPC approaches [28], [29] can also be interesting.

ACKNOWLEDGMENT

The first author is supported by the grant ANRF/ECRG/2024/004853/ENS.

REFERENCES

- A. Norouzi, H. Heidarifar, H. Borhan, M. Shahbakhti, and C. R. Koch, "Integrating machine learning and model predictive control for automotive applications: A review and future directions," *Engineering Applications of Artificial Intelligence*, vol. 120, p. 105878, 2023.
- [2] P. K. Mishra, M. V. Gasparino, and G. Chowdhary, "Deep model predictive control with stability guarantees," *IEEE Trans. on Autom. Control*, 2025.
- [3] D. Q. Mayne, E. C. Kerrigan, E. J. Van W., and P. Falugi, "Tube-based robust nonlinear model predictive control," *Int. Journal of Robust and Nonlinear Control*, vol. 21, no. 11, pp. 1341–1353, 2011.
- [4] G. Joshi and G. Chowdhary, "Deep model reference adaptive control," in 58th Conf. on Decision and Control. IEEE, 2019, pp. 4601–4608.
- [5] T. Zieger, A. Savchenko, T. Oehlschlägel, and R. Findeisen, "Towards safe neural network supported model predictive control," in 21st IFAC world congress. IFAC, 2019.
- [6] N. Hovakimyan and C. Cao, L₁ adaptive control theory: Guaranteed robustness with fast adaptation. SIAM, 2010.
- [7] R. Sinha, J. Harrison, S. M. Richards, and M. Pavone, "Adaptive robust model predictive control with matched and unmatched uncertainty," pp. 906–913, 2022.
- [8] P. K. Mishra, D. Chatterjee, and D. E. Quevedo, "Sparse and constrained stochastic predictive control for networked systems," *Automatica*, vol. 87, pp. 40–51, 2018.
- [9] P. K. Mishra, S. S. Diwale, C. N. Jones, and D. Chatterjee, "Reference tracking stochastic model predictive control over unreliable channels and bounded control actions," *Automatica*, vol. 127, p. 109512, 2021.
- [10] T. De Bruin, J. Kober, K. Tuyls, and R. Babuska, "Experience selection in deep reinforcement learning for control," *Journal of Machine Learning Research*, vol. 19, 2018.
- [11] A. F. Handbook, "Federal aviation administration," Department of Transportation, 1972.
- [12] G. W. H. Van Es, P. J. van der Geest, and A. M. H. Nieuwpoort, "Safety aspects of aircraft operations in crosswind," 2001.
- [13] K. Albee, C. Oestreich, C. Specht, A. Terán Espinoza, J. Todd, I. Hokaj, R. Lampariello, and R. Linares, "A robust observation, planning, and control pipeline for autonomous rendezvous with tumbling targets," *Frontiers in Robotics and AI*, vol. 8, p. 641338, 2021.
- [14] A. Billard, S. Mirrazavi, and N. Figueroa, Learning for adaptive and reactive robot control: a dynamical systems approach. Mit Press, 2022.
- [15] A. Parsi, P. Anagnostaras, A. Iannelli, and R. S. Smith, "Computationally efficient robust mpc using optimized constraint tightening," in 61st Conf. on Decision and Control. IEEE, 2022, pp. 1770–1775.
- [16] T. L. M. Santos, A. D. Bonzanini, T. A. N. Heirung, and A. Mesbah, "A constraint-tightening approach to nonlinear model predictive control with chance constraints for stochastic systems," in *American Control Conf.* IEEE, 2019, pp. 1641–1647.
- [17] J. Köhler, M. A. Müller, and F. Allgöwer, "A novel constraint tightening approach for nonlinear robust model predictive control," in *American Control Conf.* IEEE, 2018, pp. 728–734.
- [18] C. Klöppelt, J. Berberich, F. Allgöwer, and M. A. Müller, "A novel constraint-tightening approach for robust data-driven predictive control," *International Journal of Robust and Nonlinear Control*, vol. 35, no. 7, pp. 2566–2587, 2025.
- [19] M. Kögel, M. Ibrahim, C. Kallies, and R. Findeisen, "Safe hierarchical model predictive control and planning for autonomous systems," *International Journal of Robust and Nonlinear Control*, vol. 35, no. 7, pp. 2658–2676, 2025.

- [20] J. A. E. Andersson, J. Gillis, G. Horn, J. B. Rawlings, and M. Diehl, "CasADi – A software framework for nonlinear optimization and optimal control," *Mathematical Programming Computation*, vol. 11, no. 1, pp. 1–36, 2019.
- [21] T. Hayakawa, W. M. Haddad, and A. Leonessa, "A Lyapunov-based adaptive control framework for discrete-time non-linear systems with exogenous disturbances," *Int. Journal of control*, vol. 77, no. 3, pp. 250–263, 2004.
- [22] P. K. Mishra, T. Wang, M. Gazzola, and G. Chowdhary, "Centralized model predictive control with distributed adaptation," in 59th Conf. on Decision and Control. IEEE, 2020, pp. 697–703.
- [23] G. Chowdhary and E. Johnson, "A singular value maximizing data recording algorithm for concurrent learning," in *American Control Conf.* IEEE, 2011, pp. 3547–3552.
- [24] M. V. Gasparino, P. K. Mishra, and G. Chowdhary, "Unmatched uncertainty mitigation through neural network supported model predictive control," in 62nd Conf. on Decision and Control. IEEE, 2023, pp. 3555–3560.
- [25] M. V. Gasparino, V. A. Higuti, A. N. Sivakumar, A. E. Velasquez, M. Becker, and G. Chowdhary, "Cropnav: a framework for autonomous navigation in real farms," in 2023 IEEE Int. Conf. on Robotics and Automation (ICRA). IEEE, 2023, pp. 11824–11830.
- [26] V. A. Higuti, A. E. Velasquez, D. V. Magalhaes, M. Becker, and G. Chowdhary, "Under canopy light detection and ranging-based autonomous navigation," *Journal of Field Robotics*, vol. 36, no. 3, pp. 547–567, 2019.
- [27] M. J. Risbeck and J. B. Rawlings, "MPCTools: Nonlinear model predictive control tools for CasADi (octave interface)," 2016. [Online]. Available: https://bitbucket.org/rawlings-group/octave-mpctools
- [28] A. Mesbah, "Stochastic model predictive control: An overview and perspectives for future research," *IEEE Control Systems Magazine*, vol. 36, no. 6, pp. 30–44, 2016.
- [29] P. K. Mishra, J. A. Paulson, and R. D. Braatz, "Polynomial chaos-based stochastic model predictive control: An overview and future research directions," arXiv e-prints, pp. arXiv–2406, 2024. [Online]. Available: https://doi.org/10.48550/arXiv.2406.10734